ELSEVIER SCIENTIFIC PUBLISHING COMPANY, AMSTERDAM

Uranium, 1 (1982) 1—17
Elsevier Scientific Publishing Company, Amsterdam — Printed in The Netherlands

GENESIS OF SANDSTONE-TYPE URANIUM DEPOSITS IN THE SIERRA PINTADA DISTRICT, MENDOZA, ARGENTINA: A MÖSSBAUER STUDY

FELISA LABENSKI[1], HUGO B. NICOLLI[2] and CELIA SARAGOVI-BADLER[3]

[1]*Departamento de Física, Comisión Nacional de Energía Atómica, Buenos Aires (Argentina)*
[2]*Departamento de Geología Económica, Comisión Nacional de Investigaciones Espaciales, San Miguel, prov. Buenos Aires (Argentina)*, and *Consejo Nacional de Investigaciones Científicas y Técnicas, Buenos Aires (Argentina)*
[3]*Departamento de Física, Comisión Nacional de Energía Atómica, Buenos Aires (Argentina)*

(Received December 21, 1981; revised and accepted July 5, 1982)

ABSTRACT

Labenski, F., Nicolli, H.B. and Saragovi-Badler, C., 1982. Genesis of sandstone-type uranium deposits in the Sierra Pintada district, Mendoza, Argentina: a Mössbauer study. Uranium, 1: 1—18.

The genesis of sandstone-type uranium deposits in the Cochico Group (Permo-Triassic) of the Sierra Pintada district, San Rafael, Mendoza, has been studied. This is the most important uranium district in Argentina. Uranium sources, uranium transport and precipitation are discussed. Uraninite and brannerite, the main uranium minerals, occur within the matrix of sandstone.

Several phenomena can be deduced regarding the depositional environment. Where oxygen was available, precipitation of hydrated ferric oxides occurred; γ-$Fe_2O_3 \cdot nH_2O$ varieties (identified by Mössbauer spectroscopy) precipitated in the upper levels of the aquifer, where CO_2 partial pressure was lower, giving reddish or reddish-brown beds.

The CO_2 partial pressure also determines the distribution of biogenic agents such as bacteria. Bacteria thus find a more favourable environment for their development and action in upper levels of an aquifer. In the corresponding horizons local reduction occurred where UO_2 precipitated; therefore the highest uranium concentrations correspond to sandstone levels with reddish or reddish-brown pigment. These pigments have been identified by Mössbauer spectroscopy.

Selected samples were studied using Mössbauer technique at room and liquid-nitrogen temperatures. From this study four groups were distinguished. In all of them minerals of the chlorite series were identified with the Fe^{2+} ion in a distorted octahedral site.

Samples with low Fe^{3+} content correspond to grey sandstones with a small degree of alteration of beds with no evidence of uranium-bearing solutions. By contrast, samples with a higher Fe^{3+} content in chlorites also show lepidocrocite or maghemite (or hematite) and correspond to reddish or reddish-brown sandstones with a high degree of alteration and in which uranium ores occur.

INTRODUCTION

In previous papers (Nicolli, 1972; Nicolli et al., 1973, 1980), the main problems related to the genesis of sandstone-type uranium deposits in the

0167-5583/82/0000—0000/$02.75

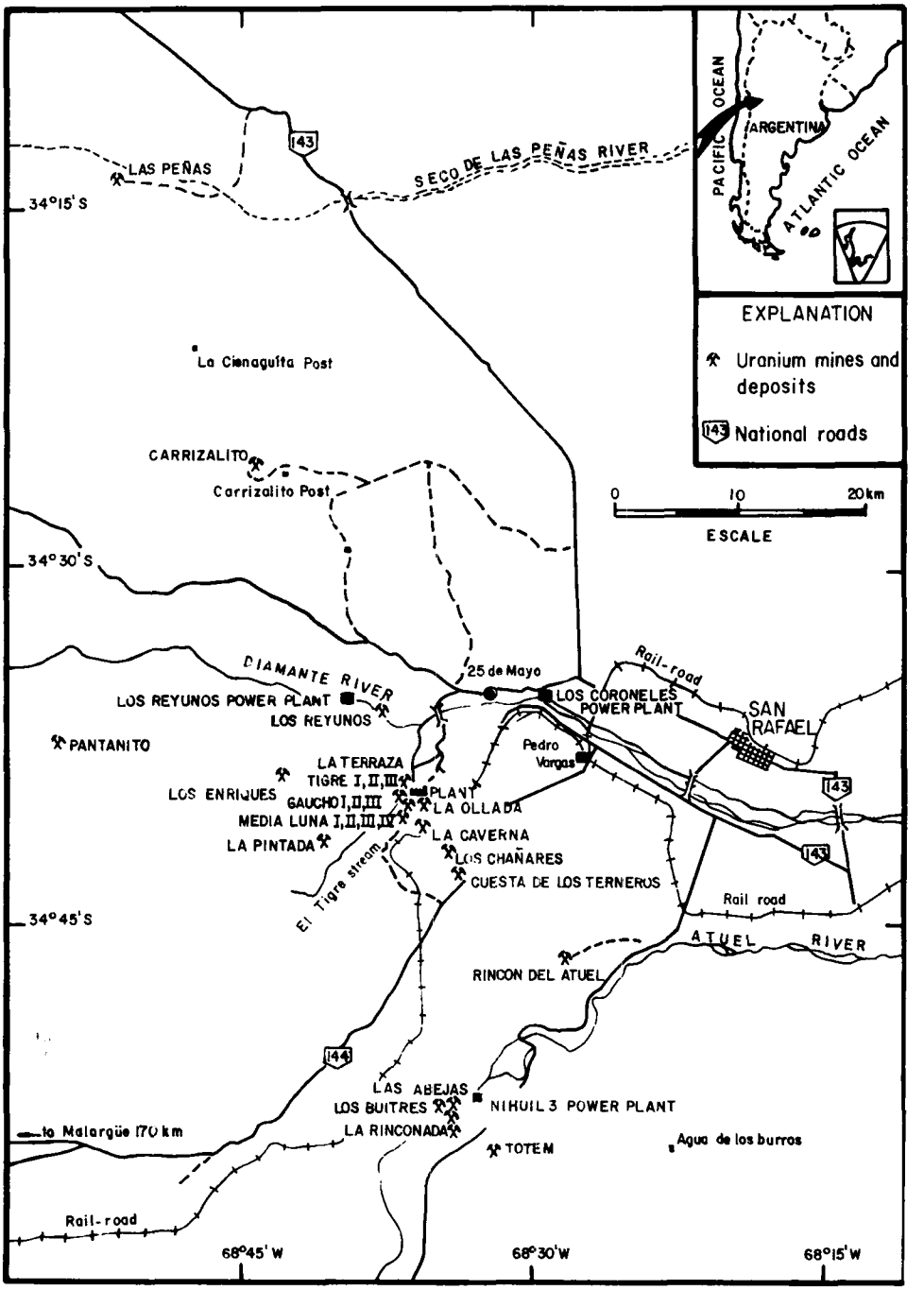

Fig. 1. Sierra Pintada uranium district, San Rafael, Mendoza, Argentina.

Sierra Pintada district, western Argentina, have been studied. Dissolution of uranium from its sources, uranium-transport phenomena and processes leading to uranium precipitation in observed host rocks have also been discussed. The latter depends on the distribution of reducing agents, bacteria being the most important agent. Bacterial development and activity are mainly regulated by the CO_2 partial pressure.

As the different pigments occurring in sandstone often reveal environmental changes, their identification is of great importance in defining the main physico-chemical characteristics of the environment. As is well known, iron oxides are commonly present in pigments. Given that Mössbauer spectroscopy has become a very useful tool in the study of iron minerals (Herzenberg and Riley, 1970; Greenwood and Gibbs, 1971), this technique was used in the present investigation to identify the different iron oxides occurring in reddish, reddish-brown and reddish-violet beds bearing high uranium contents.

Our results show the validity of the genetic model proposed for the Sierra Pintada uranium deposits referred to in the previously mentioned papers.

LOCATION AND GENERAL GEOLOGY

Sierra Pintada, situated between 69°—65°W and 33°—39°S, is a 3500-km^2 geomorphological unit, a hilly strip with relatively low slopes (Fig. 1).

The Sierra Pintada uranium district is located in the Province of Mendoza, 35 km west of the town of San Rafael, Argentina. It consists of several uranium deposits and many anomalies in a 400-km^2 area. It is presently the principal uranium district in Argentina, with reserves on the order of 16,000,000 tons of ore and with grades varying from 0.70 to 1.18% U_3O_8 (Nicolli et al., 1980).

The geology of the area has been studied by Polanski (1964), González Díaz (1964, 1972), Rodríguez and Valdiviezo (1970), Ortega Furlotti et al. (1972), Criado Roque (1972), Criado Roque and Ibáñez (1976) and Pérez (1979). For practical reasons the stratigraphic sequence established by the Comisión Nacional de Energía Atómica for the area of uranium deposits has been adopted (Fig. 2).

SAMPLING AND LABORATORY STUDIES

In the Sierra Pintada uranium district, many open-cast workings were sampled and, in strategically selected places, geological profiles and systematic samplings of lithological units were made; over 270 samples were collected. From 380 drillings, 50 were selected for laboratory analysis. The systematic mineralogical studies comprised over 50 samples; more than 350 thin sections and 40 polished sections were examined. The granulometric analysis and the sedimentological study comprised more than 130 samples. Over 400 samples were selected for chemical analysis and 11 samples for studies by Mössbauer spectroscopy (Nicolli et al., 1980).

ERA-THEM	SYSTEM	SUBSYSTEM	SERIES	GROUP	FORMATIONS and Members	LITHOLOGY and FACIES	AGE DETERMINATIONS (m.y.) (Toubes and Spikermann 1976 and 1979)
CENOZOIC	QUATERNARY		HOLOCENE PLEISTOCENE		SEVERAL FORMATIONS	Alluvial, aeolian and piedmond sediments, etc Basaltic and andesitic flows	Basalt 1,5 ± 1
	TERTIARY	NEOGENE	PLIOCENE		RIO SECO DEL ZAPALLO	Mainly fine grained sandstones (Intercalated basaltic and andesitic sheets)	Basalt 3,2 ± 1
			MIOCENE		AISOL	Mainly sandstones	Basalt 13 ± 0
						PENEPLANATION	
MESOZOIC	TRIASSIC		UPPER MIDDLE LOWER		PUESTO VIEJO	Massive succession of continental sediments	Granodiorite porphyry 192 ± 6
						DISCONFORMITY	
	PERMIAN - TRIASSIC			CERRO CARRIZALITO GROUP	CERRO CARRIZALITO	Rhyodacitic - rhyolitic facies	Rhyolite porphyry 219 ± 15 Rhydacite porphyry 223 ± 10 Granite porphyry 238 ± 10 Rhyolite 241/244 ± 10 Granophyre 247 ± 10
					AGUA DE LOS NOQUES	Dacitic facies	
	?				QUEBRADA DEL PIMIENTO	Basaltic facies	Basalt porphyry 259/260 ± 10 Granophyre 262 ± 10
						UNCONFORMITY	
PALEOZOIC				COCHICO GROUP	ARROYO PUNTA DEL AGUA	Mainly reddish sandstones and conglomerates	
						UNCONFORMITY	
	PERMIAN		LOWER		YACIMIENTO LOS REYUNOS — Vieja Gorda Tuff Member	Mainly crystallolithic tuffs	Crystallolithic tuff 272 ± 10
					YACIMIENTO LOS REYUNOS — Atigradas Sandstones Member	Fine to coarse - grained arkoses	
					YACIMIENTO LOS REYUNOS — Psephitic Member	Mainly conglomerates and fanglomerates	
						UNCONFORMITY	
	CARBONIFEROUS		UPPER		CERRO COLORADO	Mainly conglomerates	Andesite 281 ± 10 Micratonalite 285 ± 10
			LOWER		EL IMPERIAL	Seacoast and continental sediments	
	DEVONIAN				LA HORQUETA	Mainly marine sediments	Schist 353 ± 15

Fig. 2. Sierra Pintada uranium district: simplified stratigraphic sequence (from Nicolli et al., 1980).

Mössbauer spectroscopy with ^{57}Fe, based on the recoilless resonant interaction between gamma rays and nuclei, has been applied in identification of iron oxides and hydroxides. This is more sensitive than X-ray diffraction. In Mössbauer spectroscopy, the small shifts and splittings of nuclear-energy levels produced by different environments at various nuclear sites may be used to study mineral structures. The intensities of resonant transitions between levels serve to determine the population of nuclei in the various environments. In particular, an analysis of the characteristic patterns appearing in an ^{57}Fe absorption spectrum indicates the iron minerals present, the charge state of the iron ions in these minerals and the iron content in them.

The mineralogical determinations carried out by Arcidiacono and Saulnier (1979) comprised macroscopic studies, heavy-liquid separations, detailed studies of polished sections supplemented by microchemical tests, X-ray diffraction, X-ray fluorescence and electron microprobe analysis. These studies led to the determination of an interesting mineral association where uranium minerals (uraninite, brannerite, uranophane and coffinite), as well as sulfides (mainly pyrite and lesser amounts of arsenopyrite, chalcopyrite, bornite and marcasite) were found. These minerals were accompanied by clastic rutile, titano-magnetite, zircon, barite and apatite, and also by anatase, siderite, dolomite, calcite, hematite, other ferric oxides and clay minerals (montmorillonite, illite and kaolinite). Organic matter associated with uranium minerals was present. The main characteristics of some of the uranium minerals and anatase are described below (Nicolli et al., 1980):

Uraninite is probably the most abundant uranium mineral in the deposits. It mostly occurs in the sandstone matrix, where it may surround clasts or traverse them in the form of filling and replacement veinlets. The term uraninite is used with reference to its morphology, since it occurs in well-developed subhedral to tabular crystalline forms, skeleton or veinlike shapes. However, this uraninite shows low thorium and cerium contents and a high calcium content, which are common features of UO_2 when precipitated as pitchblende (colloform variety). The average size of the tabular crystals is 150 μm.

Brannerite commonly occurs associated with anatase and organic matter. It appears in tabular forms and round aggregates of up to 250 μm diameter. The variability in its hazel-grey internal reflections and reflectivity is associated with little compositional variation when in association with anatase. In this connection it is interesting to note the different degrees of replacement of anatase by brannerite. The electron microprobe analysis shows the presence of subrounded anatase with incipient replacement by brannerite in its core, grading up to a pseudomorphosis of brannerite after anatase.

Anatase is a common mineral. It usually occurs in the form of subrounded polycrystalline aggregates or small single subhedral crystals of a size close to 150 μm. The presence of uranium was corroborated by electron microprobe thus proving an incipient centripetal replacement.

Coffinite occurs in the matrix of the host rock cementing the clasts, in the form of crystalline aggregates associated with uraninite, pyrite and organic matter.

MÖSSBAUER SPECTROSCOPY

Mössbauer spectra for 11 sandstone samples were obtained using an Elron Mössbauer spectrometer in a transmission geometry with a 25 mCi source of ^{57}Co in a Pd matrix. Spectra were displayed on a multichannel analyzer operated in time mode. Samples in powder form containing approximately 10 mg cm^{-2} iron were used. Measurements were carried out at room and liquid-nitrogen temperatures. The first two measurements of samples were obtained by visual reduction from the raw plotted data (Nicolli, 1972; Frank et al., 1973). Spectra of the other samples (Saragovi-Badler et al., 1974, and present paper) were least-square fitted using a pure Lorentzian shape and constraining the corresponding peaks (Bunbury, 1974). The quality of each computer fit was checked by a χ^2 test, and only those of lower value were accepted. The isomer shift (I.S.) values are quoted relative to ^{57}Co in a Pd matrix at room temperature. The measured hyperfine parameters at room and liquid-nitrogen temperatures are listed in Tables I and II, respectively.

As shown in Figs. 3, 4 and 5, the experimental spectra at room temperature of samples ee39022, 219/49 and 219/116 (Fig. 3) were resolved into one doublet, while samples 219/77, 219/94, ee34107, 737/78 and ee39074 (Fig. 4) gave rise to spectra consisting of two doublets. For samples ee34106, 219/64 and 219/02 (Fig. 5) the Mössbauer spectra are more complex. They are resolved into two doublets and a magnetic structure. These samples were also measured at liquid-nitrogen temperature and the corresponding spectra

TABLE I

Mössbauer parameters at room temperature

SAMPLE	LOCATION		1st DOUBLET		2nd DOUBLET		SUPERIMPOSED HYPERFINE SPECTRA			COLOURING	REFERENCES
			Q.S (mm/s)	I.S (Pd) (mm/s)	Q.S. (mm/s)	I.S (Pd) (mm/s)	ε* (mm/s)	I.S. (mm/s)	H (Koe)		
737/78	Core sample 353 m deep	☼	1.78(2)	1.06(1)	0.48(8)	0.09(4)				Light reddish	Nicolli et al., 1980
ee39074	Core sample 66m deep	△	2.07(1)	1.04(1)	0.70(2)	0.06(1)				Light reddish-brown	Nicolli et al., 1980
ee39022	Core sample 573m deep	⊕	2.58(1)	0.98(1)						Grey	Nicolli et al., 1980
219/49	Core sample 42.9m deep	⊕	2.62(1)	0.94(2)						Grey	Saragovi-Badler et al., 1974
219/64	Core sample 63.9m deep	⊕	2.56(8)	0.93(3)	0.87(2)	0.08(2)	0.0(8)	0.11(1)	495(10)	Reddish-brown	Nicolli et al., 1973
219/77	Core sample 77.4m deep	⊕	2.58(1)	0.98(2)	0.74(3)	0.09(3)				Grey,olive-grey	Saragovi-Badler et al., 1974
219/94	Core sample 94.2m deep	⊕	2.62(1)	0.97(1)	0.83(1)	0.05(1)				Grey,olive-grey	Nicolli et al., 1973
219/102	Core sample 101.6 m deep	⊕	2.44(9)	0.85(5)	0.77(9)	0.02(1)	0.09(6)	0.14(6)	504(8)	Reddish	Saragovi-Badler et al., 1974
219/116	Core sample 116.3 m deep	⊕	2.62(1)	0.97(1)						Grey	Saragovi-Badler et al., 1974
ee34107	Surface (trenching)		2.50	1.04	0.70	0.19				Grey,ochre	Nicolli, 1972
ee34106	Surface (trenching)		2.54	1.02	0.76	0.12	0.2	0.36	515	Red-violet	Nicolli, 1972

*$\varepsilon = e^2 Q q / 8$ ☼ Borehole 906 △ Borehole 110 ⊕ Borehole 219

TABLE II

Mössbauer parameters at liquid-nitrogen temperature

SAMPLE	1st DOUBLET		2nd DOUBLET		SUPERIMPOSED HYPERFINE SPECTRA			U_3O_8	RADIOMETRY	REFERENCES
	Q.S. (mm/s)	I.S.(Pd) (mm/s)	Q.S. (mm/s)	I.S.(Pd) (mm/s)	ε* (mm/s)	I.S. (mm/s)	H (Koe)	(%)	(c/s)	
737/78	2.00(2)	1.15(1)	0.69(10)	0.10(7)				n.d.	480	Nicolli et al., 1980
ee39074	2.55(2)	1.06(1)	0.72(8)	0.20(10)				0.20	n.d.	Nicolli et al., 1980
ee39022	2.81(1)	1.1 (1)						0.0002	n.d.	Nicolli et al., 1980
219/49	2.76(6)	1.06(1)						0.0006	n.d.	Saragovi-Badler et al., 1974
219/64	2.5 (1)	1.1 (1)	0.85(3)	0.09(3)	0.07(9)	0.3(1)	527(15)	0.30	600	Nicolli et al., 1973
219/77	2.7 (1)	1.0 (1)	0.75(3)	0.09(3)				n.d.	n.d.	Saragovi-Badler et al., 1974
219/94	2.78(1)	1.01(1)	0.8 (1)	0.06(1)				0.0009	40	Nicolli et al., 1973
219/102	2.60(4)	0.94(3)	0.81(6)	0.05(2)	0.14(5)	0.22(1)	518(1)	0.046	n.d.	Saragovi-Badler et al., 1974
219/116	2.73(1)	0.99(1)	0.8 (1)	0.04(3)				0.0006	n.d.	Saragovi-Badler et al., 1974

*$\varepsilon = e^2 Q q/8$ n.d. = non determined

exhibit the same characteristics as those corresponding to room temperature*.

It is well known that there is a relation between the area of each component of a Mössbauer spectrum and the concentration of the corresponding phase. Therefore the Fe^{3+}/Fe^{2+} ratios were calculated on the assumption that all the phases present have the same factor f, which gives the magnitude of the Mössbauer effect probability (Muir, 1968). Table III shows the Fe^{3+}/Fe^{2+} paramagnetic ratios and the contribution of each paramagnetic iron to the total iron content. The values were calculated from the spectra at room temperature and are consistent with those calculated at liquid-nitrogen temperature.

The Mössbauer parameters corresponding to the doublet present in samples ee39022, 219/49 and 219/16 indicate the presence of a Fe^{2+} ion belonging to a mineral of the chlorite series. The quadrupole splitting (Q.S.) values at room and liquid-nitrogen temperature point out a distortion in the Fe^{2+} octahedron (Bancroft et al., 1967; Malysheva et al., 1977). The line widths (Γ) of the Fe^{2+} doublets (0.4—0.5 mm s^{-1}) may be due to some inhomogeneities of the cation evironment, such as Si^{4+}, Ca^{2+}, Mn^{2+} and Mg^{2+}. In the case of sample 219/116, the appearance of the Fe^{3+} doublet at liquid-nitrogen temperature indicates that Fe^{3+} ions are present in small quantities, showing spin-spin relaxation effects.

*Liquid-nitrogen temperature spectra published in a previous paper (Saragovi-Badler et al., 1974) were fitted again using the present MANCFIT programme.

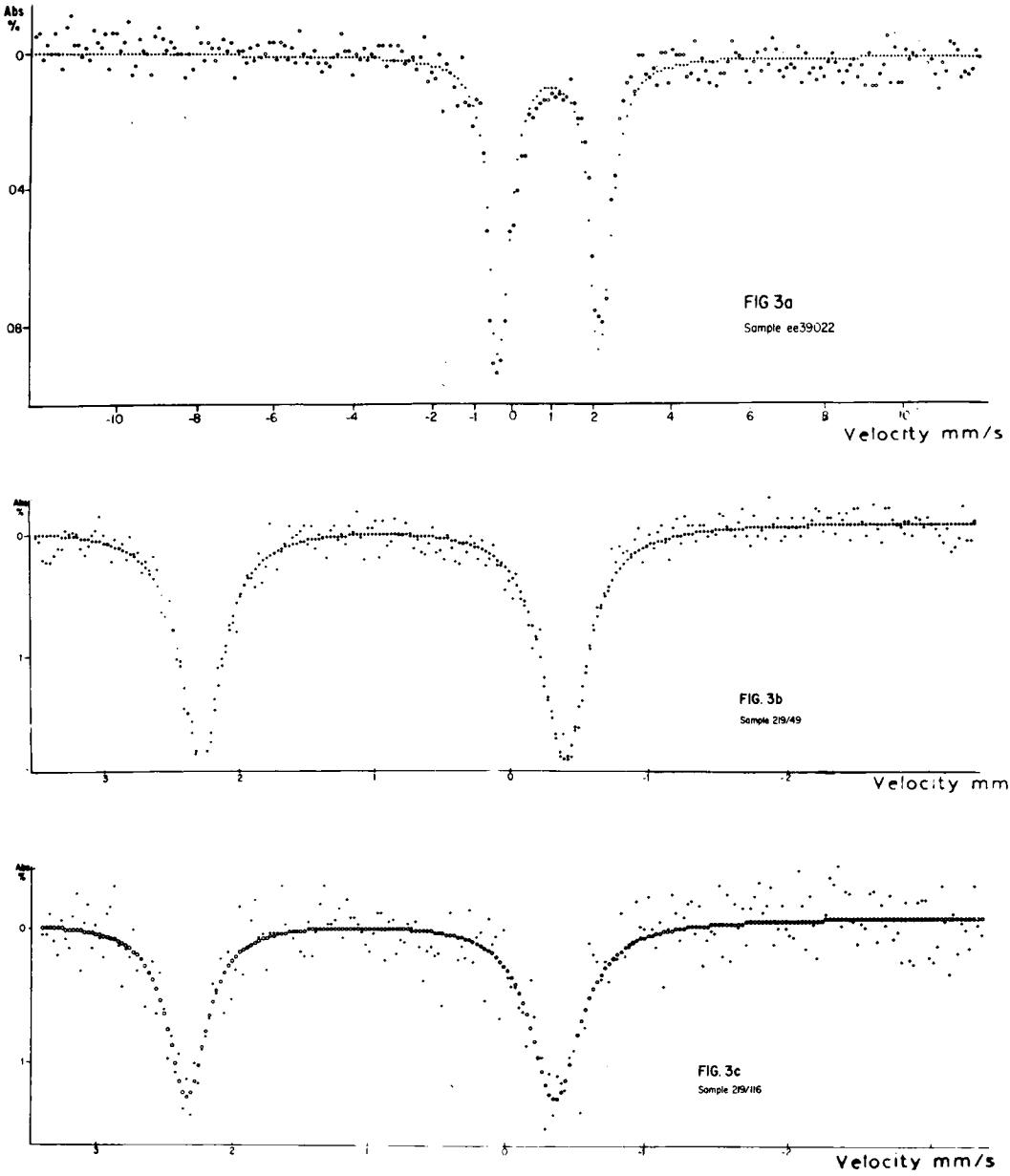

Fig. 3. Mössbauer spectra at room temperature.

The parameters of samples 219/77, 219/94 and ee34107 are compatible with Fe^{2+} and Fe^{3+} ions of a mineral of the chlorite series. The Q.S., I.S. and Γ values of the first doublet (Fe^{2+}) are similar to the two mentioned above, indicating that the environment of the Fe^{2+} ion in all these samples should

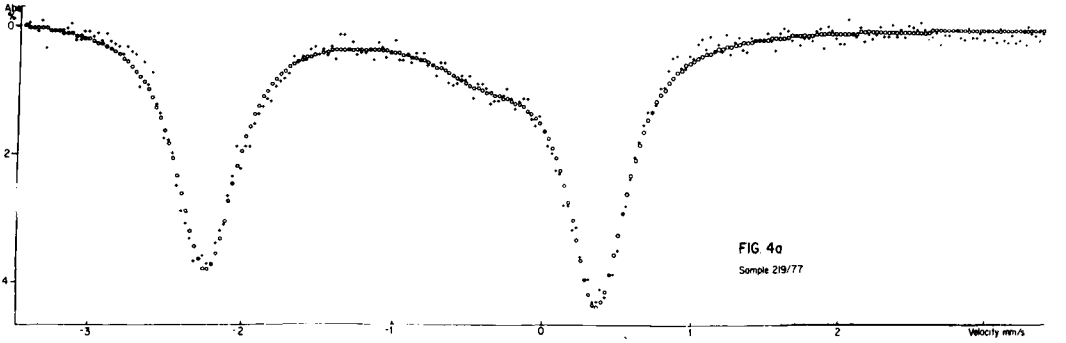

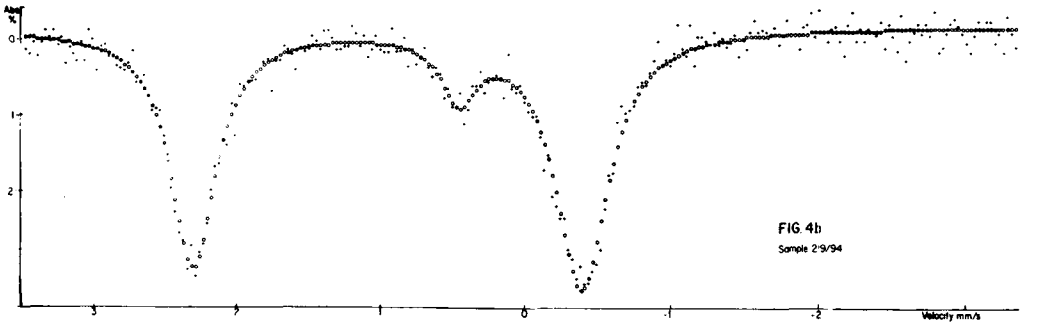

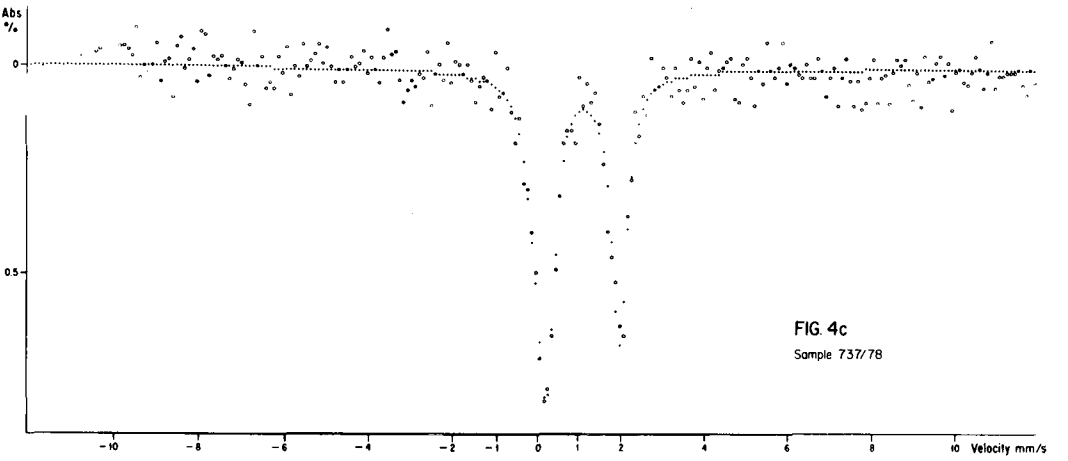

Fig. 4.a, b and c. Mössbauer spectra at room temperature.

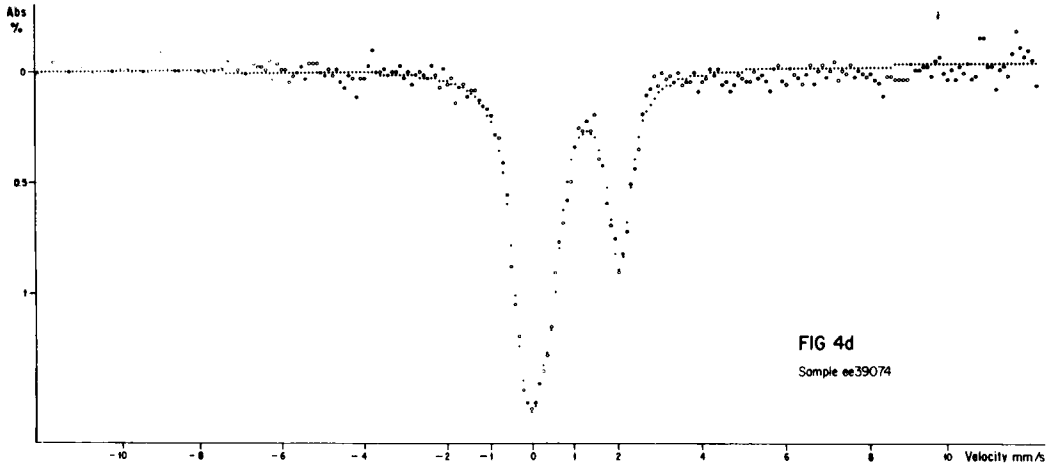

Fig. 4.d. Mössbauer spectrum at room temperature.

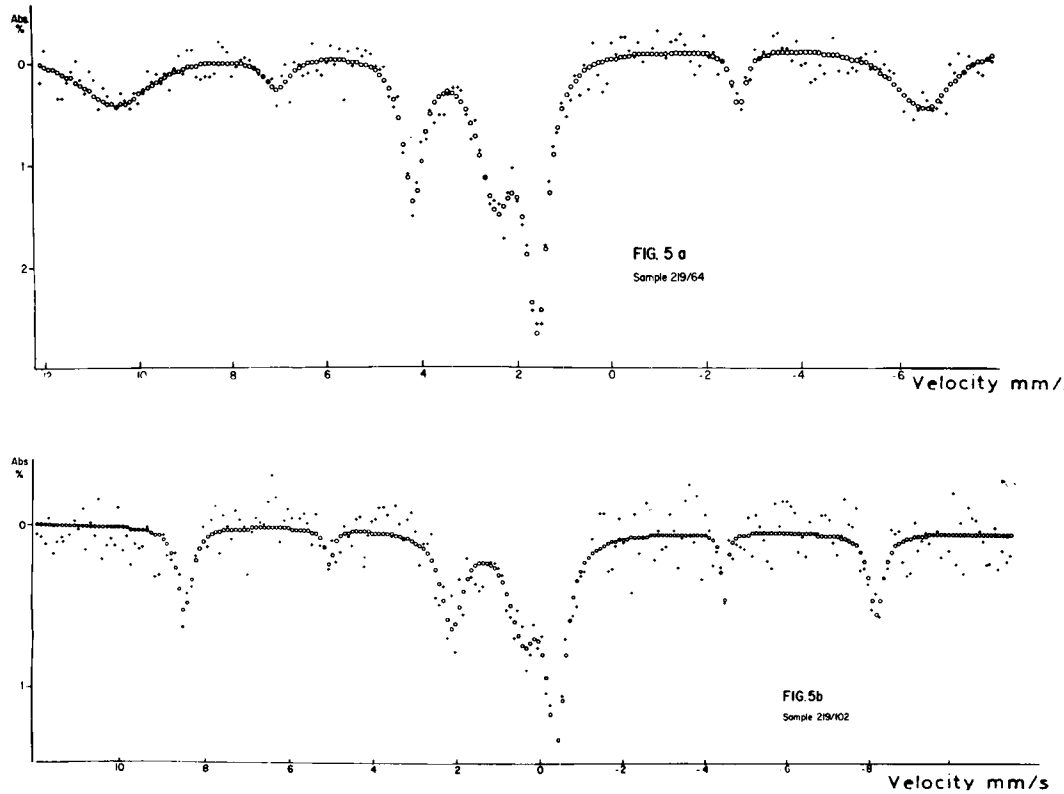

Fig. 5. Mössbauer spectra at room temperature.

TABLE III

Mössbauer Fe^{3+}/Fe^{2+} ratios at room temperature

Sample	Fe^{3+}/Fe^{2+}	$^{A}Fe^{3+}$ (%)	$^{A}Fe^{2+}$ (%)
219/77	0.35	26	74
219/94	0.20	16	84
737/78	0.22	18	82
ee39074	0.83	45	55
219/64*	1.06	51	49
219/102*	1.33	57	43

*Paramagnetic zone.

be the same. The second doublet could be assigned to a Fe^{3+} ion in an octahedral site. The value of the Q.S. indicates a distortion of the octahedra due to oxidation and the broadening of the lines (0.4—0.6 mm s^{-1}) reflects inequalities in the octahedral iron bonds. In the case of sample 219/77 it is possible that paramagnetic relaxation effects produce a more marked broadening on the line width (~0.6 mm s^{-1}) and this is reflected in a high value of the Fe^{3+}/Fe^{2+} ratio (Table III).

The first doublet of sample ee39074 spectrum indicates the presence of Fe^{2+} ion of the chlorite series. The lower value of the Q.S. suggests that the octahedral site is more distorted than in the previous samples. The second doublet of this spectrum could be assigned to a Fe^{3+} ion in the chlorite which could be ascribed to oxidation, probably caused by decomposition of the mineral OH^- groups. The possible contribution of a Fe^{3+} ion belonging to a γ-$Fe_2O_3 \cdot H_2O$ (Dézsi et al., 1969) with its lattice distorted cannot be completely excluded.

In the case of sample 737/78, the corresponding parameters of the Fe^{2+} ion doublet of the chlorite series show that the sites are still more distorted than in the latter case. The second doublet parameters could be assigned to a Fe^{3+} ion of the γ-$Fe_2O_3 \cdot H_2O$ but the Fe^{3+} possible contribution from the chlorite cannot be completely discarded.

The paramagnetic spectra parameters of samples 219/64, 219/102 and ee34106 exhibit a great similarity to the previous samples with the exception of ee39074 and 737/78. The paramagnetic Fe^{3+}/Fe^{2+} ratios are greater than 1, indicating a higher degree of oxidation. Superimposed hyperfine magnetic interactions are produced by Fe^{3+} ions of a maghemite or an hematite but our experimental values do not permit further resolution. In sample 219/63 the magnetic component is not well resolved and this may be due to a certain distribution of magnetic sites.

PIGMENTATION OF SANDSTONES

In all field studies performed on the host rock in the Sierra Pintada district, it has been noticed that the higher uranium concentrations correspond to reddish-brown or reddish-violet beds.

In general, red or reddish-brown sandstones differ from ochre sandstones, each corresponding to certain oxides or hydrated oxides of iron (Fe^{3+}) with different degrees of hydration. These oxides are common constituents of the matrix of the sandstones, usually in the form of a patina on grains of quartz and feldspars or on other principal or secondary minerals. Such oxides were precipitated from groundwaters, even into the same aquifer, to form red and ochre pigments. The red ones develop as a patina on the surface and the ochre ones precipitate in the deeper levels of an aquifer. It is well known that the red pigments correspond to γ-$Fe_2O_3 \cdot H_2O$, *lepidocrocite*, and the ochre pigments to α-$Fe_2O_3 \cdot H_2O$, *goethite*. The reason for the γ-varieties of ferric oxide appearing on the surface and the α-varieties at deeper levels, arises from these facts: Hofer and Weller (1947) proved experimentally that sand mixed with an iron-salt solution, exposed to air at 50° C, gives a reddish synthetic sandstone; the same sand immersed in the same solution and at the same temperature gives a synthetic sandstone with ochre pigments. In 1929, Albrecht (cited by Hofer and Weller, 1947) studied the oxidation of ferrous bicarbonate in a solution, concluding that while in the midst of the solution an ochre pigment gradually precipitates, a brown patina is produced on the surface. This phenomenon is favoured by the increase of the air—solution interface area.

On the other hand, a low CO_2 concentration favours the formation of γ-$Fe_2O_3 \cdot H_2O$ vs. α-$Fe_2O_3 \cdot H_2O$ in the aquifer (Nicolli, 1972). However, lepidocrocite is unstable, turning into γ-Fe_2O_3, *maghemite* (red pigment). Maghemite is, in turn, metastable and slowly becomes α-Fe_2O_3, *hematite* (red pigment). It has been assumed that in the case of the Sierra Pintada district the reddish, reddish-brown or reddish-violet beds (high uranium contents) were due to partial decomposition or transformation of lepidocrocite into the above-mentioned ferric oxides (Nicolli, 1972; Nicolli et al., 1973).

GENESIS OF THE URANIUM DEPOSITS

For the analysis of the main problems related to the genesis of sandstone-type uranium deposits in the Sierra Pintada district, three factors were considered: (a) uranium source; (b) uranium transport phenomena; and (c) uranium precipitation.

In the Sierra Pintada district there is no evidence of the action of ascendent hydrothermal solutions. The study of local structures has revealed that faults displace the uranium ore; this shows that they belong to a later age, probably contemporaneous with the Sierra Pintada block fracturing which occurred in the Late Tertiary (Nicolli et al., 1973).

The analyses of tuff samples which have revealed very low uranium contents and the devitrification processes observed in the originally vitreous material give rise to the assumption that overlying tuffs, adjacent tuffs, and/or intercalated tuffs have been important uranium sources.

The host rock (Atigradas sandstone member of the Cochico Group) is arkose, using this term in a general sense (total feldspar >15%). The arkose is characterized by lithic clasts of volcanic origin. Plagioclase (oligoclase-andesine) prevails over orthoclase. A weak kaolinization is rather extended; sericitization is not very important and chloritization appears with various degrees of intensity. Carbonatization is a typical alteration process which mainly affects feldspars in various degrees ranging from weak partial attacks to complete clast replacement in some of the samples studied. There is a regular proportion of carbonates (2—10% $CaCO_3$). Quartz is almost clean and shows fractured crystals. Perfect bipyramidal crystalline forms provide evidence for effusive rocks at the source. Apatite and zircon are common accessory minerals.

Matrix composition is similar to that of the coarse fractions. Its alteration is mainly argillaceous and similar to feldspar alteration, that is, rather intense carbonatization and chloritization with weak sericitization. Minor amounts of organic matter (<0.1%) show an irregular distribution in the matrix. Scarce cementing material consisting of recrystallized clay minerals and carbonates with minor amounts of sericite and silica have been observed. Ferric oxides are an important cementing agent in red samples. The alteration (devitrification) of the volcanic glass in lithic clasts may have also released uranium which in a second stage was redistributed throughout the uranium-bearing sandstone (Nicolli et al., 1973, 1980).

The leached uranium entered the cycle of groundwater to be redistributed together with other elements (Ca, Fe, CO_3^{2-}, etc.). These uranium-bearing solutions moved through the Atigradas sandstone aquifer. The high permeability of the rock due to the lack of consolidation (incipient diagenesis) helped this groundwater-circulation process. The underlying "red conglomerate" (under the Atigradas sandstone) with intercalated pelitic levels served as a base for the water table, thus facilitating the process. In this sense, it is interesting to observe that the distribution of reddish, reddish-brown and reddish-violet pigments corresponds to more or less horizontal beds which are parallel to the base of the water table. Such distribution *does not depend* on the spatial distribution of sandstone clasts which exhibit different characteristics (size, shape, composition, alteration type and intensity, etc.; Nicolli et al., 1980).

In that environment the mobility of uranium was facilitated by the formation of carbonate complex ions, mainly UDC, uranyl dicarbonate $[UO_2(CO_3)_2(H_2O)_2]^{2-}$, and UTC, uranyl tricarbonate $[UO_2(CO_3)_3]^{4-}$. Both are very stable, UDC prevailing at pH < 6.5 and UTC prevailing at pH > 6.5; they can give rise to the migration of important amounts of uranium. The stability of the UDC and the UTC complexes depends on the physico-

chemical conditions of the environment, mainly on pH, Eh and CO_2 partial pressure in uranium-bearing solutions. Any important changes in the values of these parameters could produce the decomposition of the complex ions and the subsequent precipitation of UO_2 (Nicolli et al., 1973, 1980).

Local low-temperature reduction processes may be inferred in the host rock. In order to establish the nature of these processes, variations of the redox potential values (Eh) must be considered. These are mainly determined by the liberation of S^{2-} ion in the oxidation of sulphides. This process is regulated by the original sulphide content of the host rock and by the possibility of bacterial development. These bacteria find a more adequate environment for development in the upper levels of an aquifer because CO_2 partial pressure is lower there than elsewhere, thus giving rise to a reduction zone where UO_2 precipitates.

As has been mentioned, formation of reddish, reddish-brown and reddish-violet pigments was favoured by lower CO_2 potential pressure, its spatial distribution being coincident with higher uranium concentrations. A remarkable fact is that the uranium ore horizons and the phreatic water base are parallel (Nicolli et al., 1973, 1980).

DISCUSSION

Samples shown in Tables I, II and III have been divided in four groups according to their common characteristics:

First group: samples 219/49; ee39022 and 219/116.

According to Mössbauer spectroscopy, a mineral of the chlorite series has been identified with the Fe^{2+} ion in a distorted octahedral site and with inhomogeneities. A very small amount of Fe^{3+} is present only in sample 219/116. These samples correspond to beds of gray sandstone with a small degree of alteration. No contribution of uranium-bearing solutions was observed (low radiometry and U_3O_8 values).

Second group: samples 219/77 and 219/94 (see also sample ee34107 in Nicolli, 1972).

Mössbauer spectroscopy parameters reveal the existence of minerals of the chlorite series. The Fe^{2+} ion is in a distorted octahedron and the amount of Fe^{3+} ion is somewhat greater than in the first group. Samples have been taken from grey to olive-grey sandstone beds with a small degree of alteration. No contribution of uranium-bearing solutions was observed (low radiometry and U_3O_8 values).

Third group: samples ee39074 and 737/78.

As in the previously mentioned groups, minerals of the chlorite series are present but in this case the octahedral Fe^{2+} sites are very distorted. In samples 737/78, γ-$Fe_2O_3 \cdot H_2O$ is observed while in ee39074, the Fe^{3+} ion could be ascribed to a chlorite or to γ-$Fe_2O_3 \cdot H_2O$. These samples correspond to light reddish or light reddish-brown sandstones which have been taken from altered beds where the occurrence of uranium ores was verified. The corresponding radiometry and U_3O_8 values are high.

Fourth group: samples 219/64 and 219/102 (see also sample ee34106 in Nicolli, 1972).

In this case a mineral of the chlorite series is observed again with the Fe^{2+} ion in a distorted octahedral site. The Fe^{3+}/Fe^{2+} ratios of the chlorite point out that very considerable oxidation took place. Furthermore maghemite (or hematite) has been identified. These samples have been taken from reddish sandstone beds with a high degree of alteration in which the occurrence of uranium ores was observed (high to very high radiometry and U_3O_8 values).

In summary, in samples of the first two groups the sole iron mineral identified belongs to the chlorite series (with the Fe^{2+} site distorted). There is a rather low Fe^{3+}/Fe^{2+} ratio. These results are concurrent with the fact that the minerals of the horizons from which the samples were taken show a lower degree of alteration (weathering) and no contribution of mineralizing solutions.

On the other hand, samples from the last two groups show, in addition to the chlorites (with the Fe^{2+} site very distorted), the occurrence of the γ varieties of ferric oxides. These results are in agreement with the fact that samples belong to horizons where the common sandstone minerals have been altered due to mineralizing solutions flowing through the sandstone aquifer. These solutions modified the Fe^{3+}/Fe^{2+} ratio (> 1) due to oxidation. In this environment local reduction phenomena (biogenic activity) which caused uranium precipitation are observed.

CONCLUSIONS

The experimental results confirm the hypothesis of the existence of physico-chemical phenomena in the depositional environment which depend mainly on the CO_2 partial pressure and which regulate the distribution of the reduction agents in it.

Consequently, the biogenic action (bacterial development) was limited to the uranium host sandstone only at the upper levels of the free aquifer. There, the CO_2 partial pressure is lower, facilitating the bacterial development which produced a locally reducing environment where uranium minerals precipitate. At the same horizons, γ-$Fe_2O_3 \cdot H_2O$ (lepidocrocite) occurs since this variety precipitates only at a low value of CO_2 partial pressure.

Lepidocrocite is unstable and turns to maghemite which slowly becomes hematite. Thus the occurrence of these ferric oxides in the depositional environment is coincident with the highest uranium concentrations.

Satisfactory agreement was obtained between experimental data and the genetic model for sandstone-type uranium deposits in the Sierra Pintada district.

ACKNOWLEDGEMENTS

The authors want to express their appreciation to the authorities of the Comisión Nacional de Investigaciones Espaciales (CNIE) for their support

and interest in the subject. The authors also want to convey their appreciation to the staff of the Sección Geoquímica and the División Estudios Especiales of the Comisión Nacional de Energía Atómica, and the staff of the Departamento de Geología Económica, CNIE, for their cooperation.

REFERENCES

Arcidiacono, E. and Saulnier, M.E., 1979. Estudio sobre la asociación mineral de los yacimientos y manifestaciones de uranio del área de Sierra Pintada, San Rafael, Mendoza. CNEA, Tech. Int. Rep. NO. 1479 D.E.E. 12/79, 18 pp.

Brancroft, G.M. Maddock, A.G. and Burns, R.G., 1967. Applications of the Mössbauer effect to silicate mineralogy. I. Iron silicates of known crystal structure. Geochim. Cosmochim. Acta, 31: 2219—2246.

Bunbury, D.St.P., 1974. Programme "MANCFIT". Schuster Lab., Univ. of Manchester.

Criado Roque, P., 1972. Bloque de San Rafael. In: A.F. Leanza (Editor), Geología Regional Argentina. Acad. Nac. Ciencias, Córdoba, pp. 283—295.

Criado Roque, P. and Ibáñez, G., 1976. Provincia geológica Sanrafaelino—Pampeana. In: Segundo Simposio de Geología Regional Argentina. Acad. Nac. Ciencias, Córdoba, I: 837—869.

Dézsi, I., Vertes, A. and Kiss, L., 1969. Mössbauer study of the corrosion products of iron. J. Radioanal. Chem., 2: 183—189.

Frank, E., Labenski, F. and Saragovi-Badler, C., 1973. Mössbauer spectroscopy of iron compounds present in uranium containing sandstones. Radiochem. Radioanal. Lett., 14: 349—356.

González Díaz, E.F., 1964. Rasgos geológicos y evolución geomorfológica de la Hoja 27-d (San Rafael) y zona occidental vecina (Provincia de Mendoza). Asoc. Geol. Arg. Rev., XIX: 151—188.

González Diaz, E.F., 1972. Descripción geológica de la Hoja 27-d, San Rafael. Serv. Nac. Geol. Min. Bol., 132, 127 pp.

Greenwood, N.N. and Gibbs, T.C., 1971. Mössbauer Spectroscopy. Chapman and Hall, London, 659 pp.

Herzenberg, C.L. and Riley, D.L., 1970. Current Applications of Mössbauer Spectroscopy in Geochemistry. In: E.L. Grove (Editor), Developments in Applied Spectroscopy, VIII. Plenum Press, New York, N.Y., pp. 177—291.

Hofer, L.J.E. and Weller, S., 1947. The nature of the iron compounds in red and yellow sandstone. Science, 14, p. 470.

Malysheva, T.V., Satarova, L.M. and Polyakova, N.P., 1977. Thermal transformations of layered silicates and the nature of the iron bearing phase in the CII-Type Murray carbonaceous chondrite. Geochem. Int., 14: 117—128. (Geokhimiya, 8: 1136—1148).

Muir Jr., A.H., 1968. Analysis of complex Mössbauer Spectra by stripping techniques. In: I.J. Gruverman (Editor), Mössbauer Effect Methodology, IV. Plenum Press, New York, N.Y., pp. 75—102.

Nicolli, H.B., 1972. Consideraciones sobre la génesis de depósitos uraníferos en areniscas: distrito de Sierra Pintada, departamento de San Rafael, provincia de Mendoza (República Argentina). Actas V Congress Geol. Argentino, Buenos Aires, 1974, II: 223—242.

Nicolli, H.P., Chaar, E. and Latorre, C.O., 1973. Características génesis de los yacimientos nucleares "Dr. Baulíes" y "Los Reyunos", departamento San Rafael, provincia de Mendoza. Bol. Acad. Nac. Ciencias, Córdoba, 50: 147—166.

Nicolli, H.B., Gamba, M.A. and Ferreyra, R.E., 1980. Geochemical characteristics and genesis of sandstone-type uranium deposits, Sierra Pintada district, San Rafael, Mendoza, Argentina. Proc. 26th Int. Geol. Congress, Paris, Section 13, Theme 2.2, Metallogenesis of Uranium. Geoinstitut, Beograd, pp. 163—187.

Ortega Furlotti, A., Rodriguez, E.J., Prieto, A.O. and Valvidiezo, A., 1972. El nuevo distrito uranífero de Sierra Pintada, provincia de Mendoza, Actas V Congress Geol. Argentino, Buenos Aires, 1974, II: 267—284.

Pérez, E., 1979. Geología del Bloque de San Rafael. In: Curso Latinoamericano de Evaluación de Indicios Uraníferos. CNEA—CIEN, II, CNEA-AC-22/79, 12 pp.

Polanski, J., 1964. Descripción geológica de la Hoja 26-c, La Tosca. Direc. Nac. Geol. y Min. Bol., 101, 86 pp.

Rodríguez, E.J. and Valdiviezo, A., 1970. Exploración geológica semiregional. Sierra Pintada. CNEA, Tech. Int. Rep. NO. 418, 40 pp.

Saragovi-Badler, C., Labenski, F. and Frak, E., 1974. Mössbauer spectroscopy of iron compounds present in the profile of an uranium deposit. J. Phys., 35: C6-563—C6-568.

Toubes, R.O. and Spikermann, J.P., 1976. Algunas edades K/Ar para la Sierra Pintada, provincia de Mendoza. Asoc. Geol. Arg. Rev., XXXI: 118—126.

Toubes, R.O. and Spikermann, J.P., 1979. Nuevas edades K/Ar para la Sierra Pintada, provincia de Mendoza. Asoc. Geol. Arg. Rev., XXXIV: 73—79.